OAK RIDGE NATIONAL LABORATORY
operated by
UNION CARBIDE CORPORATION
for the
U.S. ATOMIC ENERGY COMMISSION

ORNL-TM-663

ISOTOPES DEVELOPMENT CENTER REPORT

CYCLOTRON-PRODUCED RADIOISOTOPES (I)

T. A. Butler
J. J. Pinajian

ORNL-TM-663

Contract No. W-7405-eng-26

ISOTOPES DEVELOPMENT CENTER REPORT

CYCLOTRON-PRODUCED RADIOISOTOPES (I)

T. A. Butler
J. J. Pinajian

Isotopes Division

Date Issued

OCT 28 1963

OAK RIDGE NATIONAL LABORATORY
Oak Ridge, Tennessee
operated by
UNION CARBIDE CORPORATION
for the
U.S. ATOMIC ENERGY COMMISSION

CYCLOTRON-PRODUCED RADIOISOTOPES (I)

T. A. Butler
J. J. Pinajian

ABSTRACT

A study of the internal proton beam characteristics of the ORNL 86-Inch Cyclotron has shown that, for (p,n) reactions, the yield can be used as a function of beam power to optimize production yields. The method of varying the proton energy over the range of 17-23 Mev is described. The radial distribution (radial width, ~1/4 in.), beam spread (by autoradiography), and penetration (stacked foil experiments at 6° to the incident beam) are examined. The penetration of 23-Mev protons in Fe [$Fe^{56}(p,n)Co^{56}$ + $Fe^{57}(p,2n)Co^{56}$ + $Fe^{58}(p,3n)Co^{56}$], Ni [$Ni^{58}(p,2p)Co^{57}$ + $Ni^{58}(p,pn + p,2n)Ni^{57}$—36 hr⟶$Co^{57}$], Cu [$Cu^{65}(p,n)Zn^{65}$] and Rh [$Rh^{103}(p,n)Pd^{103}$ and $Rh^{103}(p,pn)Rh^{102}$] was used to study low energy (p,n) and high energy (p,2n), (p,pn) or (p,3n) reactions. Optimum target thickness was 0.006 in. for single nucleon evaporation processes and ~0.003 in. for two and three nucleon evaporation processes.

INTERNAL BEAM CHARACTERISTICS, FLAT PLATE TARGETS

For increased efficiency in the production of neutron-deficient radioisotopes in the ORNL 86-Inch Cyclotron, it is desirable to have knowledge of the beam characteristics, e.g. spatial distribution (both internal beam and external beam), beam energy, and the power input. With this knowledge, target yields may be optimized and contamination from other radioisotopes minimized. In this report the characteristics of the internal proton beam impinging on a flat plate target[1] is examined and its relationship to the production of radioisotopes considered.

Yield as a Function of Beam Power

With the protons of ~20 Mev energy, the thick target yield of a particular isotope will increase with increasing proton energy. This increase is due to the fact that the reaction cross section does not drop to zero after peaking (but decreases to ~10% of the peak value with an increase of 3-4 Mev in proton energy). If the cross section were to drop to zero, the yield would remain constant with increasing proton energy.

Green and Martin[2] have calculated thick target yields for the reactions $Cu^{65}(p,n)Zn^{65}$ and $Cu^{63}(p,2n)Zn^{62}$ from excitation functions measured with the ORNL 86-Inch Cyclotron. The energy dependence of the yield from a

---

[1] T. A. Butler, Reactor- and Cyclotron-Produced Isotopes, July-October, 1962, ORNL-TM-463.

[2] F. L. Green and J. A. Martin, Nuclear Sci. and Eng. 7, 387 (1960).

typical (p,n) reaction is shown in Fig. 1. Curve A shows the slow increase above 15 Mev in Zn^{65} yield when plotted in mc/ma-hr, whereas Curve B shows that the yield reaches a peak at ~15 Mev and then drops when plotted as a function of beam power on the target. Since target characteristics limit the total beam which may be utilized because of the power dissipation problem, the important consideration becomes the yield per kw-hr rather than the yield per ma-hr. A typical (p,2n), thick target, production rate is given in Fig. 2. The yield per kw-hr and per ma-hr are both still rising steeply at 22 Mev. Therefore, maximum available energy of the protons can be utilized. Target thickness may be optimized to reduce the cost of materials or conserve materials (e.g., enriched isotopes which may be expensive or not readily available in large quantities) as well as to limit the production of unwanted activities.

Proton Energy Range

In a fixed-frequency cyclotron, a simple method of bombarding a target at an energy below the maximum design energy is to insert the target at a radius at which the desired energy can be obtained. Spacing between the dees and the gap between the pole faces severely limits exploiting the technique to any degree. The ORNL 86-Inch Cyclotron utilizes a system of precessing the orbit centers toward the target by introducing a first harmonic in the magnetic field.[3]

Auxiliary coils (asymmetric, current-carrying windings on the pole tips) installed as part of the beam deflection system, make it possible to reduce the beam energy from ~23 to ~17 Mev. Stable, large beam currents are more readily available by pushing the effective beam center toward the target to decrease the energy.

Radial Distribution

Cohen[4] has measured the radial distribution of an internal cyclotron target by mounting a stack of seventeen 1/32-in.-long carbon foils on a modified window-type target. Figure 3 shows the target head, a proton orbit which just misses the target, and the very next orbit which would strike the target. The measured activity was due to long-lived impurities in the carbon and the 20-min activity from $C^{12}(p,pn)C^{11}$. The radial width of the internal beam is ~1/4 in.; the highest beam intensity is at the top or inner portion of the target (i.e., in Fig. 4 at the 31-in. radius rather than the 31-1/4-in. radius).

Beam Spread

In Fig. 4, a flat target plate is shown tangent to the beam. The next orbit is shown striking the target with a radial increase of 1/4-in. which is, in effect, the radial width of the internal beam. In actual operation,

[3] Electromagnetic Research Div. Semiannual Progress Report for Period Ending March 20, 1953, ORNL-1531. (June 8, 1953).

[4] B. L. Cohen, Spatial Distribution of Current on an Internal Cyclotron Target, ORNL-1348 (1952).

UNCLASSIFIED
ORNL-LR-DWG. 11087

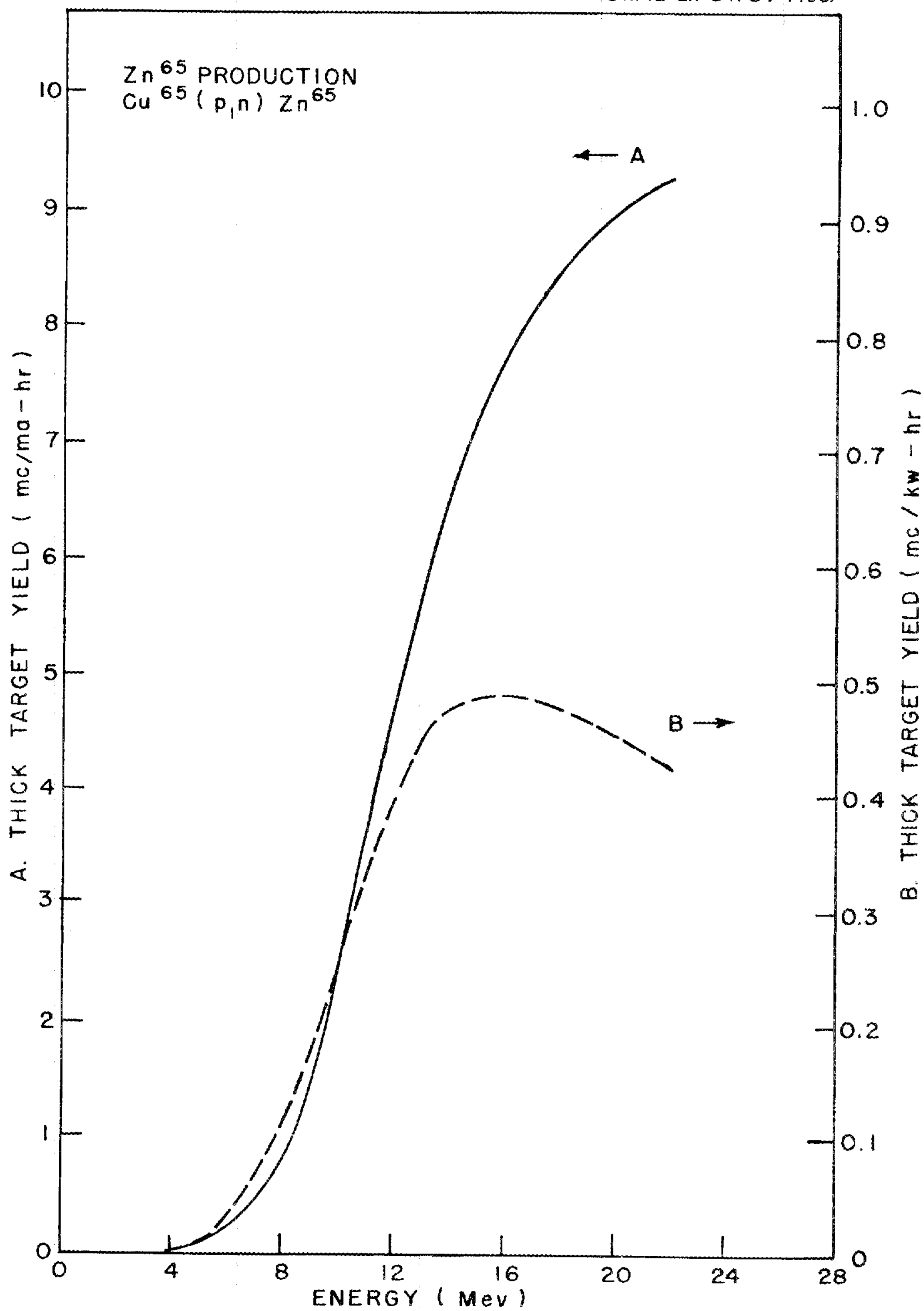

Fig. 1. ORNL 86-Inch Cyclotron Thick Target Yield of Zn^{65} Produced by $Cu^{63}(p,n)Zn^{65}$.

UNCLASSIFIED
ORNL-LR-DWG. 11088

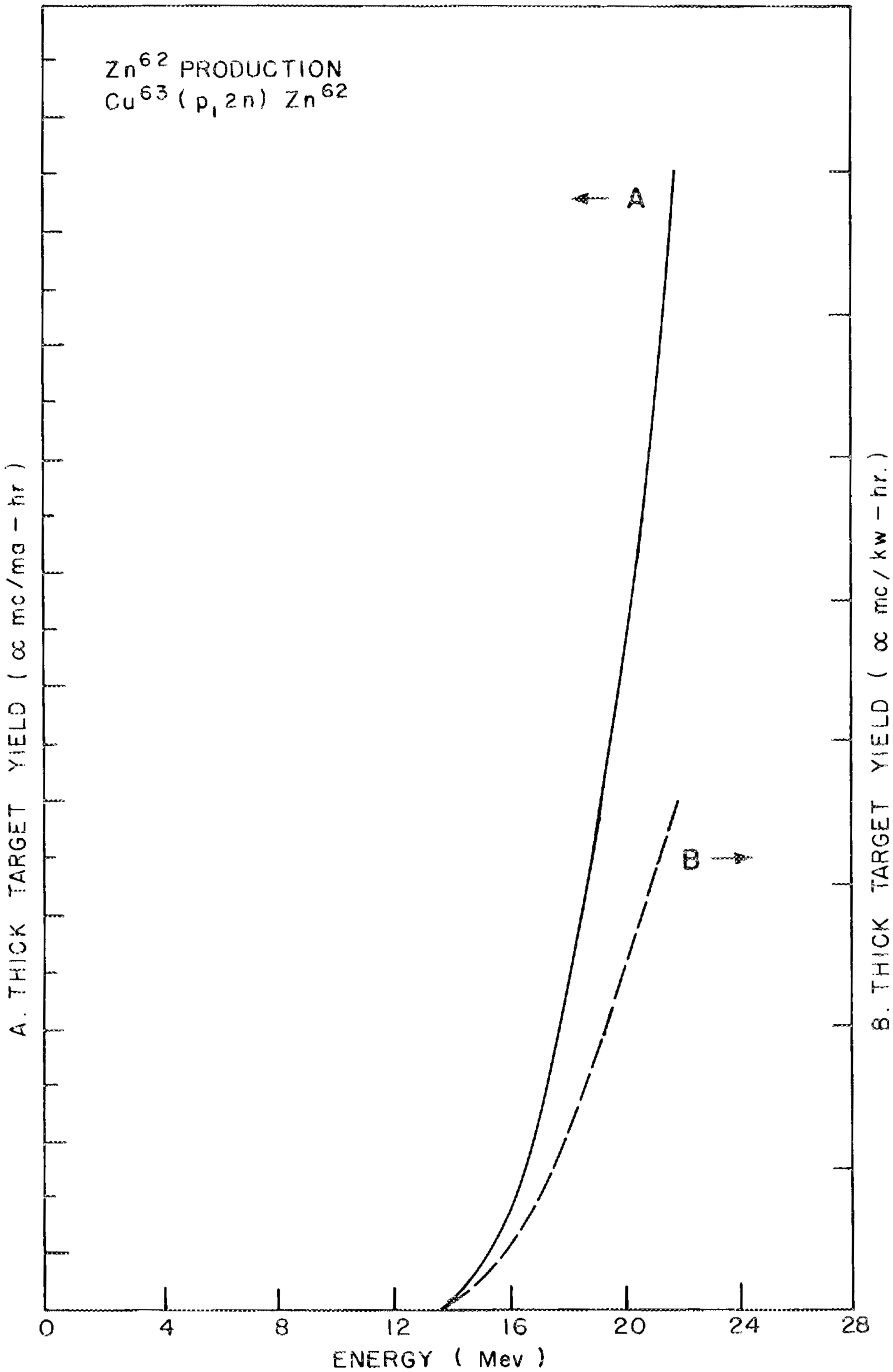

Fig. 2. ORNL 86-Inch Cyclotron Thick Target Yield of Zn^{62} Produced by $Cu^{63}(p,2n)Zn^{62}$.

UNCLASSIFIED
ORNL-LR-DWG 54227

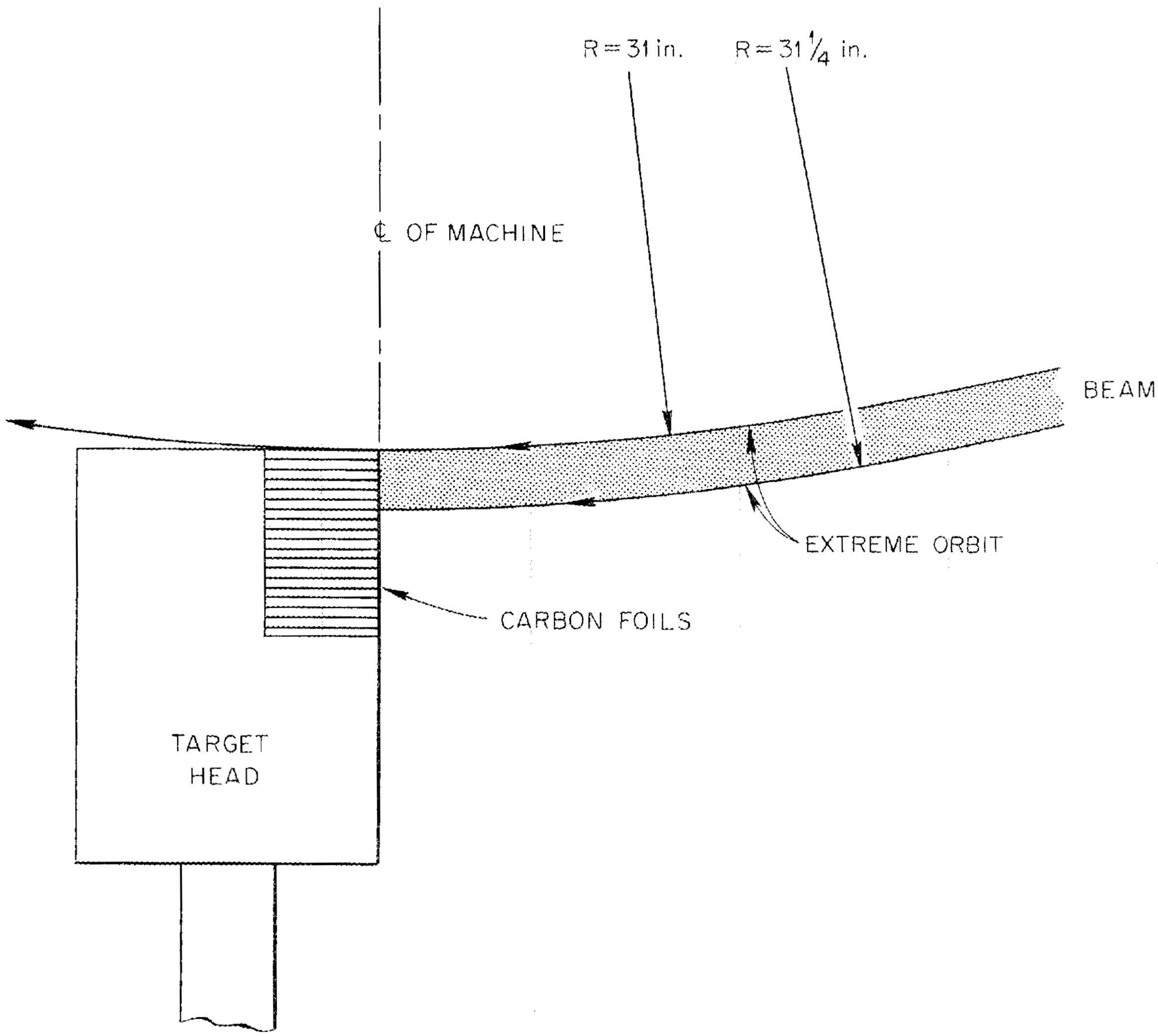

Fig. 3. ORNL 86-Inch Cyclotron Internal Probe Target and Beam Orbit.

UNCLASSIFIED
ORNL—LR—DWG 54228

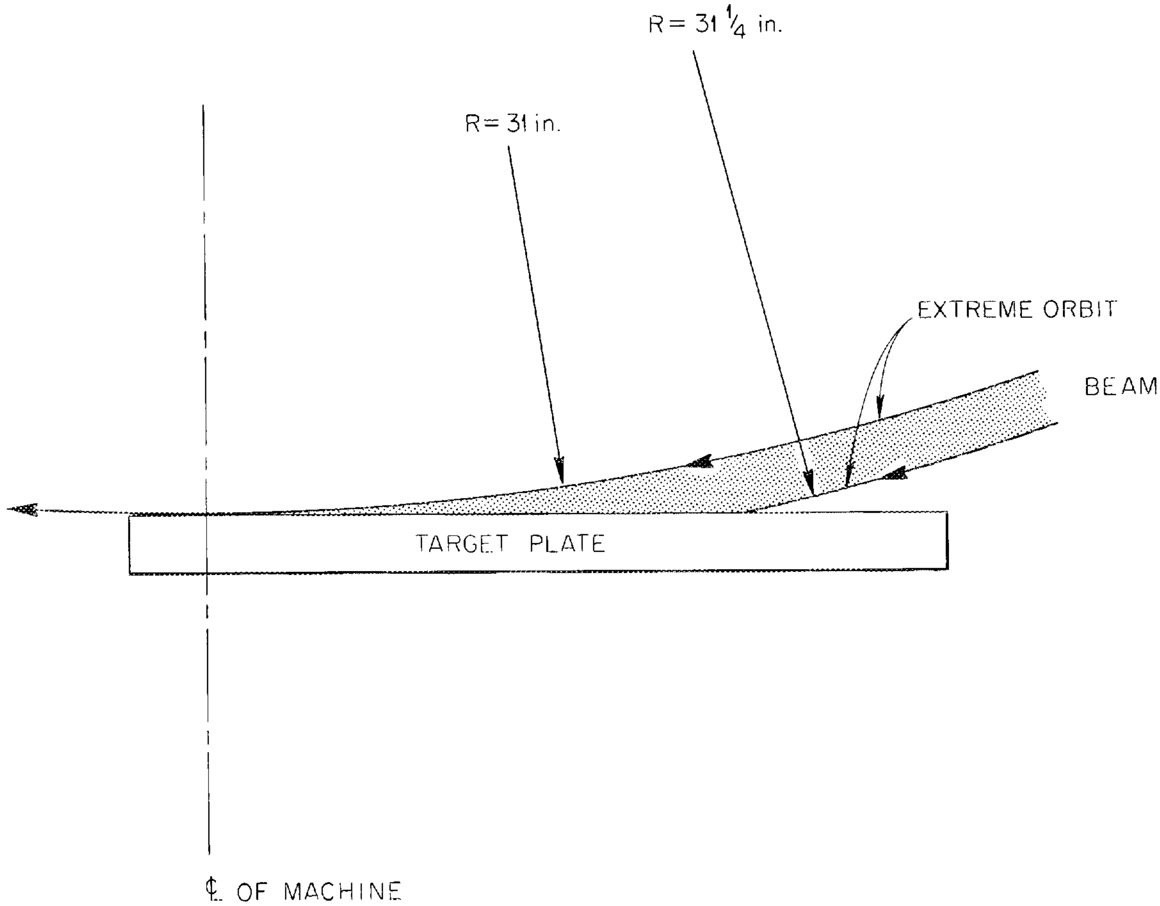

Fig. 4. ORNL 86-Inch Cyclotron Flat Plate Target and Beam Orbit.

the auxiliary field is varied periodially so that the beam will not impinge too long on one spot. An autoradiograph of a typical target is shown in Fig. 5.

Beam Penetration

A study was made of the proton beam penetration into a flat plate target material by presenting stacked foil targets at an angle of six degrees to the deflected beam at the "T" position (see Fig. 5).[1] Figure 6 shows the details of the position -- the beam enters on the right side and the target probe is inserted through the open port. A 0.375-in., water-cooled, graphite collimator is used to center the beam on the stack of ten 0.001- x 0.5- x 3.75-in. foils. (Figure 7 is a schematic presentation of the geometry.) The center 3.0 in. of the foils was exposed to the beam (~0.2 μa-hr). The foils were then set aside until the short-lived activities decayed to negligible quantities. To eliminate scattering effects, an additional 0.250 in. was cut from each end of the 3.0-in. sections.

The analyses were performed using (1) a 3.0- by 3.0-in. NaI(Tl) crystal mounted on a CBS-CL 1083 photomultiplier tube with a resolution, for Cs^{137} 0.662-Mev gamma ray, of 8.53% and (2) a 1.5- by 0.080-in. NaI(Tl) crystal mounted on a RCA 6655A photomultiplier tube with a resolution, for the Cd^{109} 22.2-kev x ray, of 36%. Former data were collected with a 512-channel pulse height analyzer, while the latter were collected with a 256-channel pulse height analyzer. The 22.2-kev Cd^{109} and 32.2-kev Cs^{137} x rays[5] were used to calibrate the thin NaI(Tl) detector. A 0.732 g/cm^2 Lucite absorber was used with the 3- by 3-in. crystal. The following activities were followed:[6]

Fe foils:	77-day Co^{56}
Cu foils:	245-day Zn^{65}
Rh foils:	17-day Pd^{103}
	210-day Rh^{102}

The 210-day Rh^{102} activity which was followed through 55 days demonstrated, within the experimental error, a half-life of 210 days.

The results of the penetration studies are shown in Figs. 8-11. For the (p,n) reactions studied, optimum thickness (i.e., a minimum thickness required to produce >95% of the desired activity in an infinitely thick target) appears to be ~0.006 in. For (p,pn), (p,2n) or (p,3n) reactions optimum thickness for the reactions studied appear to be ≤ 0.003 in. These results are summarized in Table 1.

---

[5]C. E. Crouthamel (ed.), Applied Gamma-Ray Spectrometry, Appendix IV, Pergamon Press, New York, 1960.

[6]D. Strominger, J. M. Hollander, and G. T. Seaborg, Rev. Mod. Phys. 30, 585 (1958). The decay schemes, gamma energies, and half-lifes used are from Ref. 6; where necessary, this information was brought up to date (e.g., by use of Ref. 7).

[7]J. F. Stehn, Nucleonics 18 (11), 186 (1960).

[8]T. A. Butler, Reactor- and Cyclotron-Produced Isotopes, November-December 1962, ORNL-TM-530.

UNCLASSIFIED
PHOTO 61929

Fig. 5. Autoradiograph of Aluminum Flat Plate Target Showing Beam Distribution.

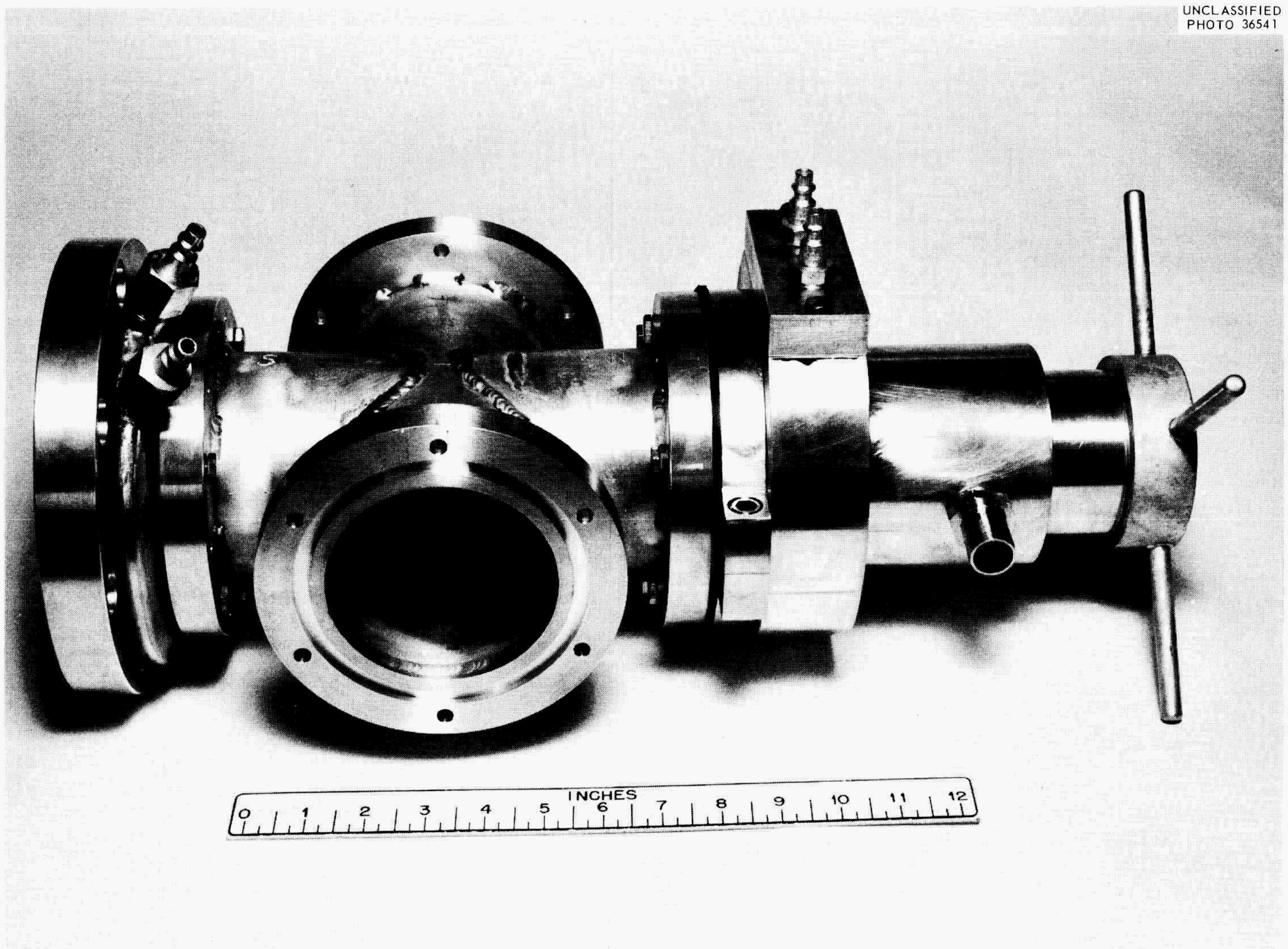

Fig. 6. ORNL 86-Inch Cyclotron "T" Position Assembly Showing Lucite Probe Ports and Water Cooled Collimators. Beam Enters at Right.

UNCLASSIFIED
ORNL-DWG 63-1475

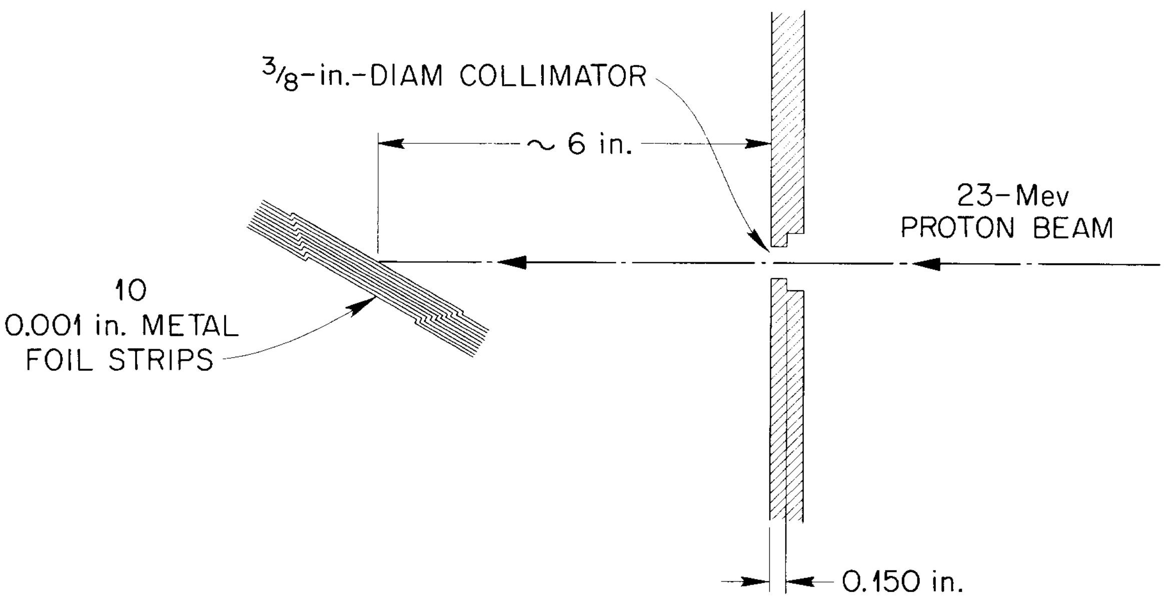

Fig. 7. Schematic Showing Presentation of Ten 0.001-in. Foil Strips to 23-Mev Proton Beam of ORNL 86-Inch Cyclotron.

UNCLASSIFIED
ORNL-LR-DWG 77967

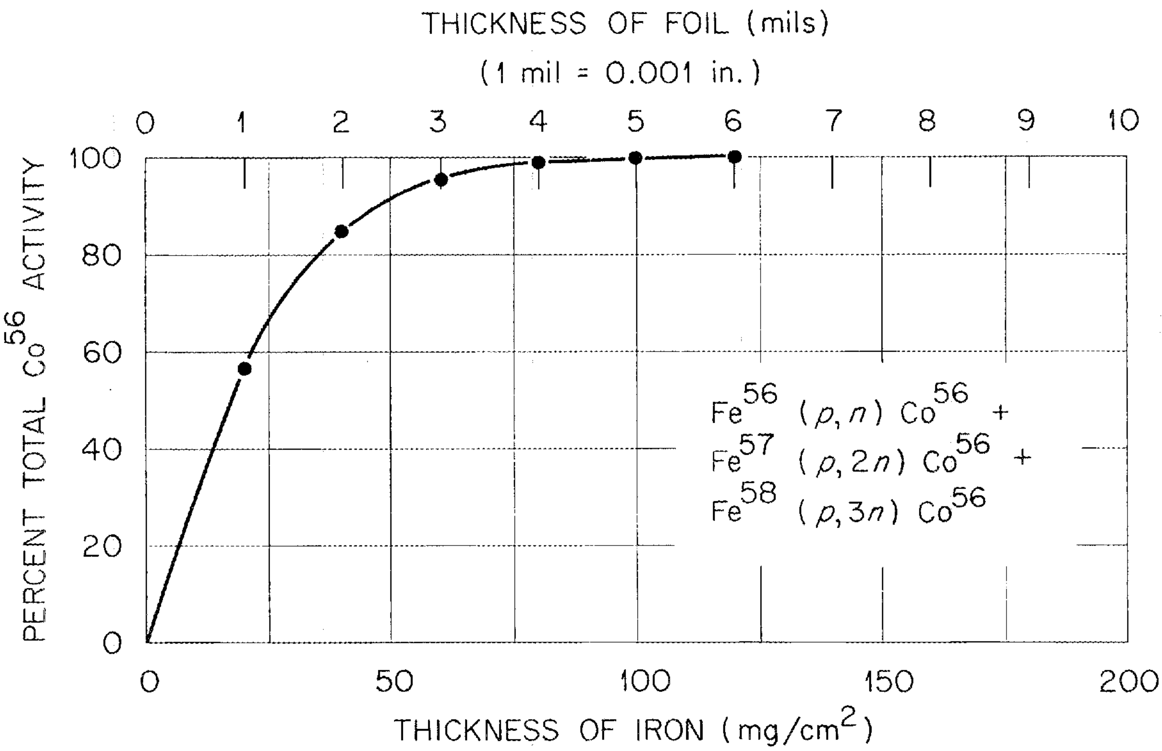

Fig. 8. Production of Co^{56} in Iron as a Function of Target Thickness With the Target at 6° to the Incident Beam.

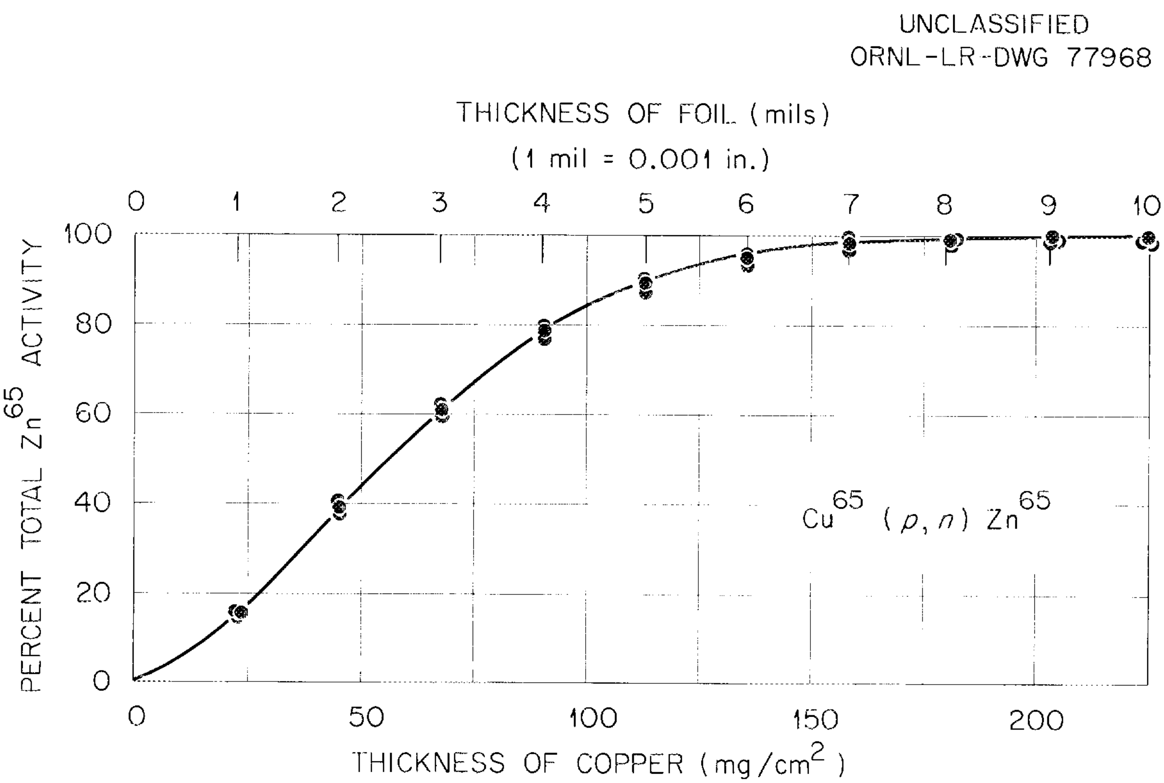

Fig. 9. Production of Zn^{65} in Copper as a Function of Target Thickness With the Target at 6° to the Incident Beam.

UNCLASSIFIED
ORNL-LR-DWG 77965

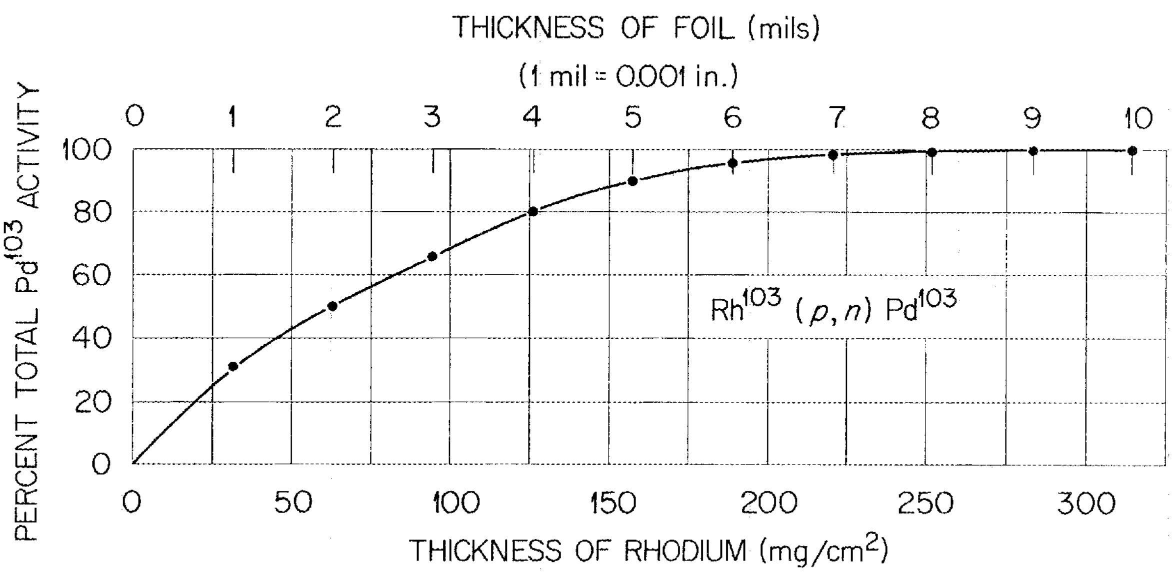

Fig. 10. Production of Pd^{103} in Rhodium as a Function of Target Thickness With the Target at 6° to the Incident Beam.

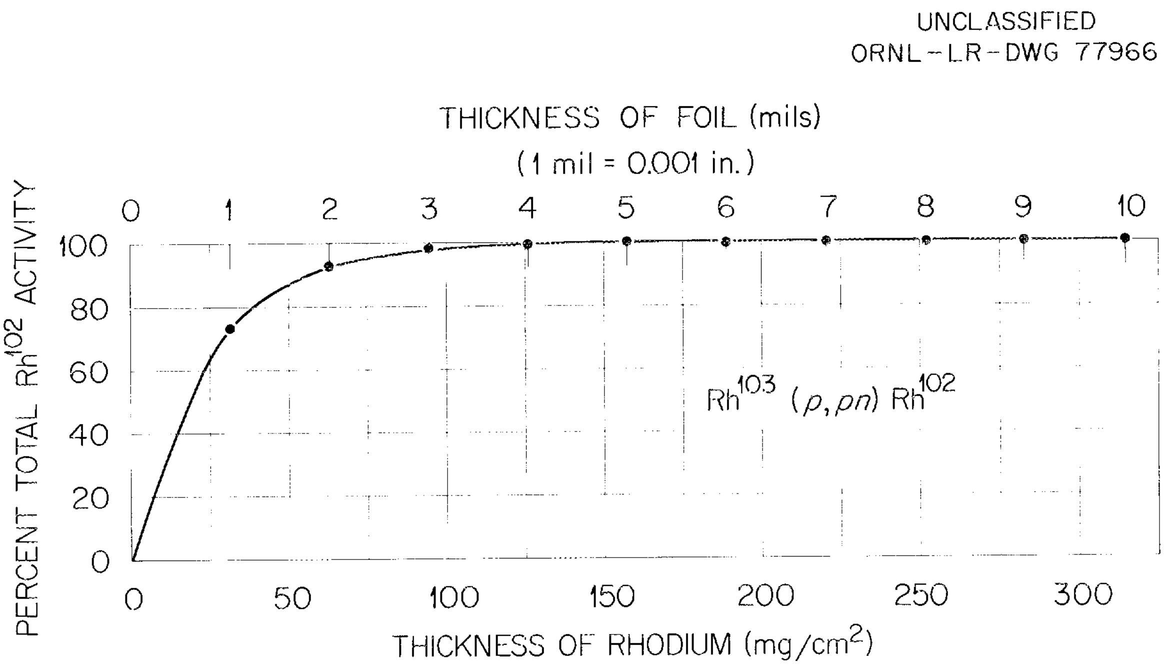

Fig. 11. Production of Rh^{102} in Rhodium as a Function of Target Thickness With the Target at 6° to the Incident Beam.

Table 1. Penetration, at 6°, of 23-Mev Protons Into Fe, Ni, Cu, and Rh

Target	Reaction	Assay	Photon Detected[h]	NaI(Tl) Crystal	Minimum Thickness (> 95% Activity) (mils)	mg/cm^2
Fe	$Fe^{56}(p,n)Co^{56}$ + $Fe^{57}(p,2n)Co^{56}$ + $Fe^{58}(p,3n)Co^{56}$	a	0.845 Mev	d	3.0	60
Ni[g]	$Ni^{58}(p,2p)Co^{57}$ + $Ni^{58}(p,pn + p,2n)Ni^{57}$ $Ni^{57} \xrightarrow{36hr} Co^{57}$	b	0.122 Mev	d	2.5	--
Cu	$Cu^{65}(p,n)Zn^{65}$	a	1.119 Mev	d	6.0	135
Rh	$Rh^{103}(p,n)Pd^{103}$	a	20.2 kev	e	6.0	190
			22.5 kev[c]	f	---	---
	$Rh^{103}(p,pn)Rh^{102}$	a	0.475 Mev	d	2.5	77
			1.08 Mev	d	2.5	77

[a]Method of assay: whole foil γ-spectroscopy.

[b]Method of assay: step-wise electrostripping and γ-spectroscopy. (Ref. 8)

[c]X-ray energy reported by independent analysis group using NaI(Tl) crystal (f).

[d]3-in. by 3-in. NaI(Tl) crystal with 0.732 g/cm^2 Lucite absorber.

[e]1.5 by 0.080 in. NaI(Tl) crystal with no absorber.

[f]3-in. by 3-in. NaI(Tl) crystal with 0.734 g/cm^2 polystyrene absorber.

[g]Ni plated copper flat plate target.

[h]Photon energies were taken from Ref. 5 and 6.

DISTRIBUTION

1. P. S. Baker
2. E. E. Beauchamp
3. G. E. Boyd
4-5. T. A. Butler
6. F. N. Case
7. L. T. Corbin
8. J. A. Cox
9. F. L. Culler
10. S. B. Ewing
11. J. H. Gillette
12. H. R. Gwinn
13. C. P. Keim
14. M. T. Kelley
15. E. H. Kobisk
16. E. Lamb
17. L. O. Love
18. W. S. Lyon
19. J. J. Pinajian
20. W. K. Prater
21. M. E. Ramsey
22. R. A. Robinson
23. A. F. Rupp
24. K. A. Spainhour
25. H. E. Seagren
26. J. A. Swartout
27. A. M. Weinberg
28. J. C. White
29. Laboratory Records - RC
30-31. Central Research Library
32-34. Laboratory Records
35. Document Reference Section

EXTERNAL DISTRIBUTION

36. P. C. Aebersold, Div. of Isotopes Development, AEC, Washington, D.C.
37. Argonne National Laboratory, Argonne, Illinois
38. A. Berman, Div. of Isotopes Development, AEC, Washington, D.C.
39. H. D. Bruner, Div. of Biology and Medicine, AEC, Washington, D.C.
40. J. T. Cristy, AEC-RLOO, Richland, Washington
41. D. C. Davis, Research and Development Div., AEC-ORO, Oak Ridge, Tenn.
42. I. A. Hobbs, AEC-SROO, Aiken, S. C.
43. J. W. Irvine, 6-426, MIT, Cambridge 39, Massachusetts
44. T. R. Jones, Div. of Research, AEC, Washington, D.C.
45. P. W. McDaniel, Div. of Research, AEC, Washington, D.C.
46. B. Manowitz, Brookhaven National Lab., Upton, L.I., N.Y.
47. R. B. Martin, Research and Development Div., AEC-ORO, Oak Ridge, Tenn.
48. Mound Laboratory, Miamisburg, Ohio
49. F. K. Pittman, Div. of Reactor Development, AEC, Washington, D.C.
50. W. H. Reas, General Electric Co., HAPO, Richland, Washington
51. H. M. Roth, Research and Development Div., AEC-ORO, Oak Ridge, Tenn.
52. L. G. Stang, Hot Lab. Div., Brookhaven National Lab., Upton, L.I.,N.Y.
53. V. R. Thayer, Atomic Energy Division, E. I. DuPont, Wilmington, Del.
54. Library, Brookhaven National Laboratory, Upton, L.I., N.Y.
55. Library, Hanford Atomic Products Operation, Richland, Washington
56. Library, Savannah River Laboratory, Aiken, S.C.
57-71. DTIE, AEC